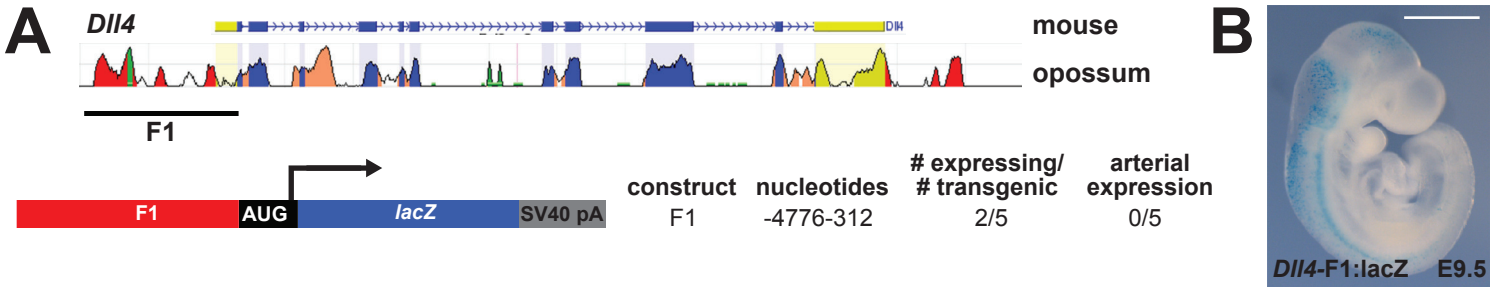

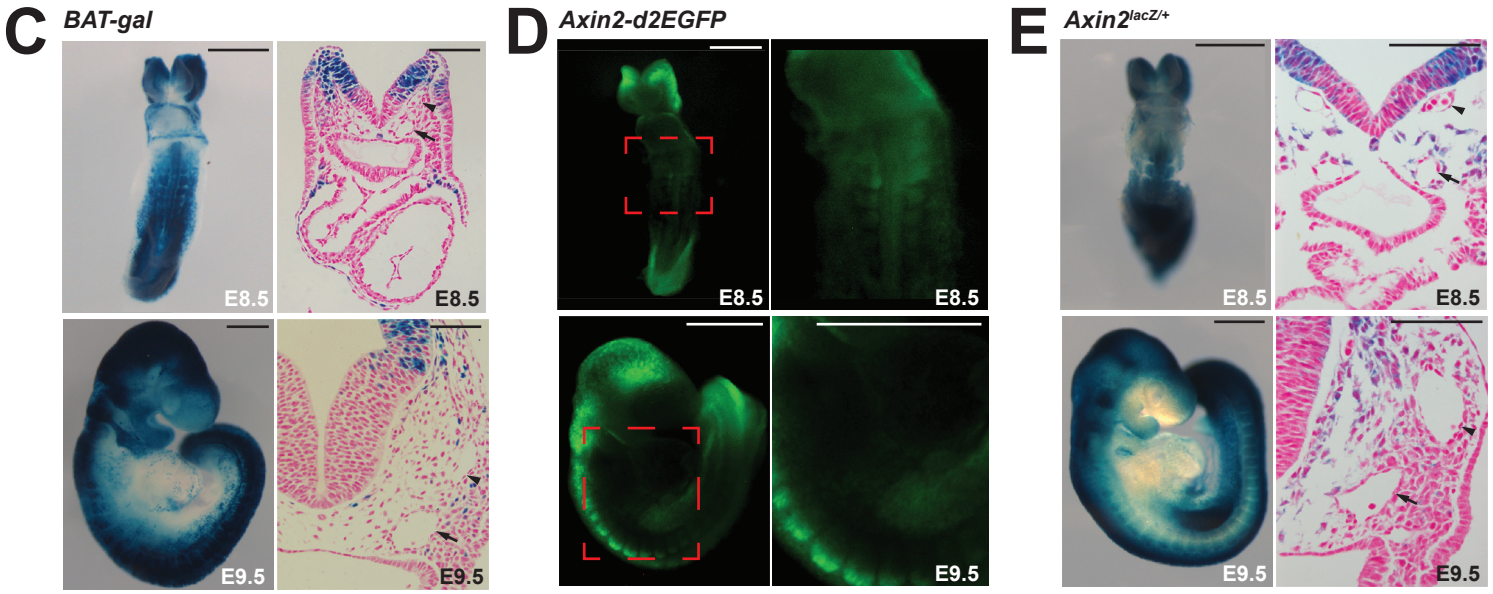

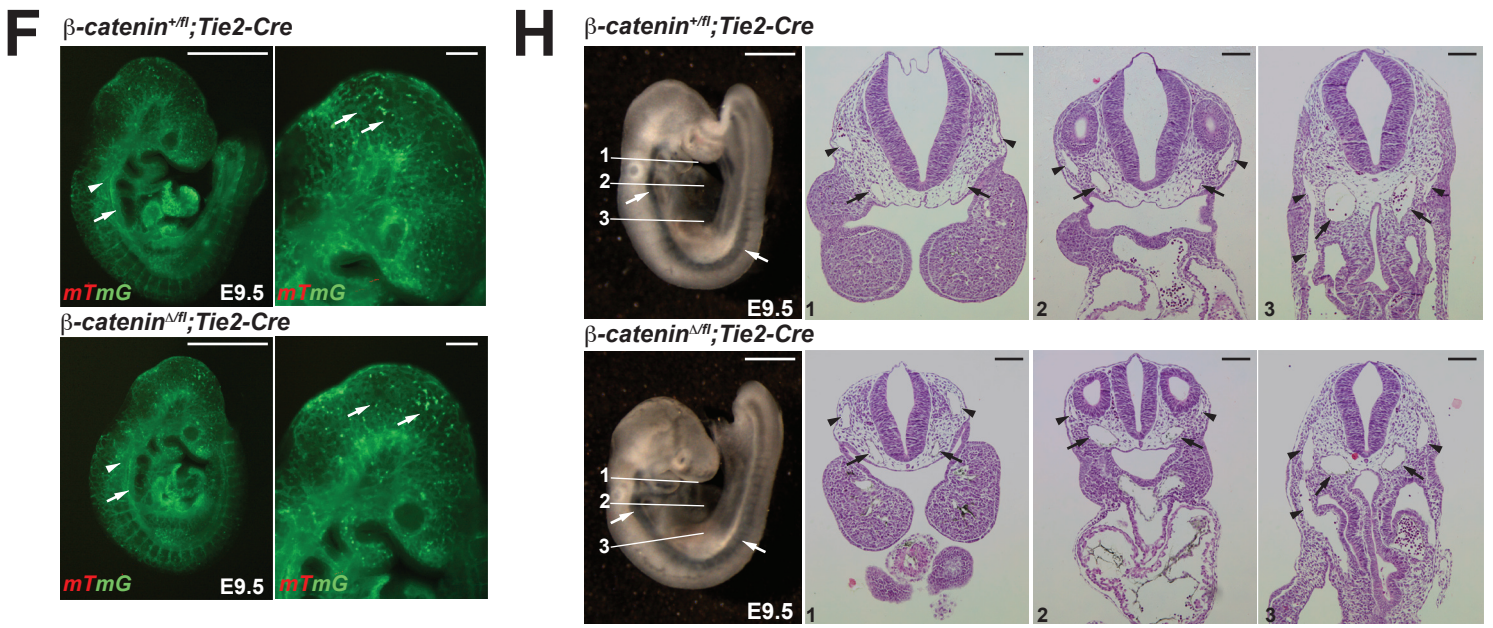

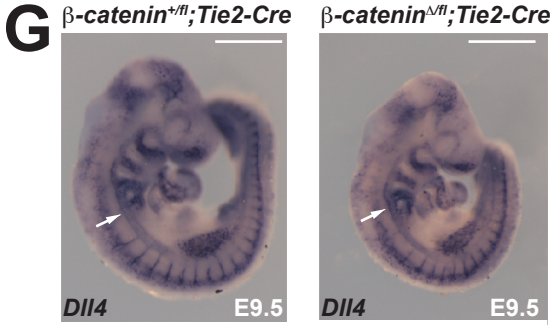

Wythe et al_Figure S1

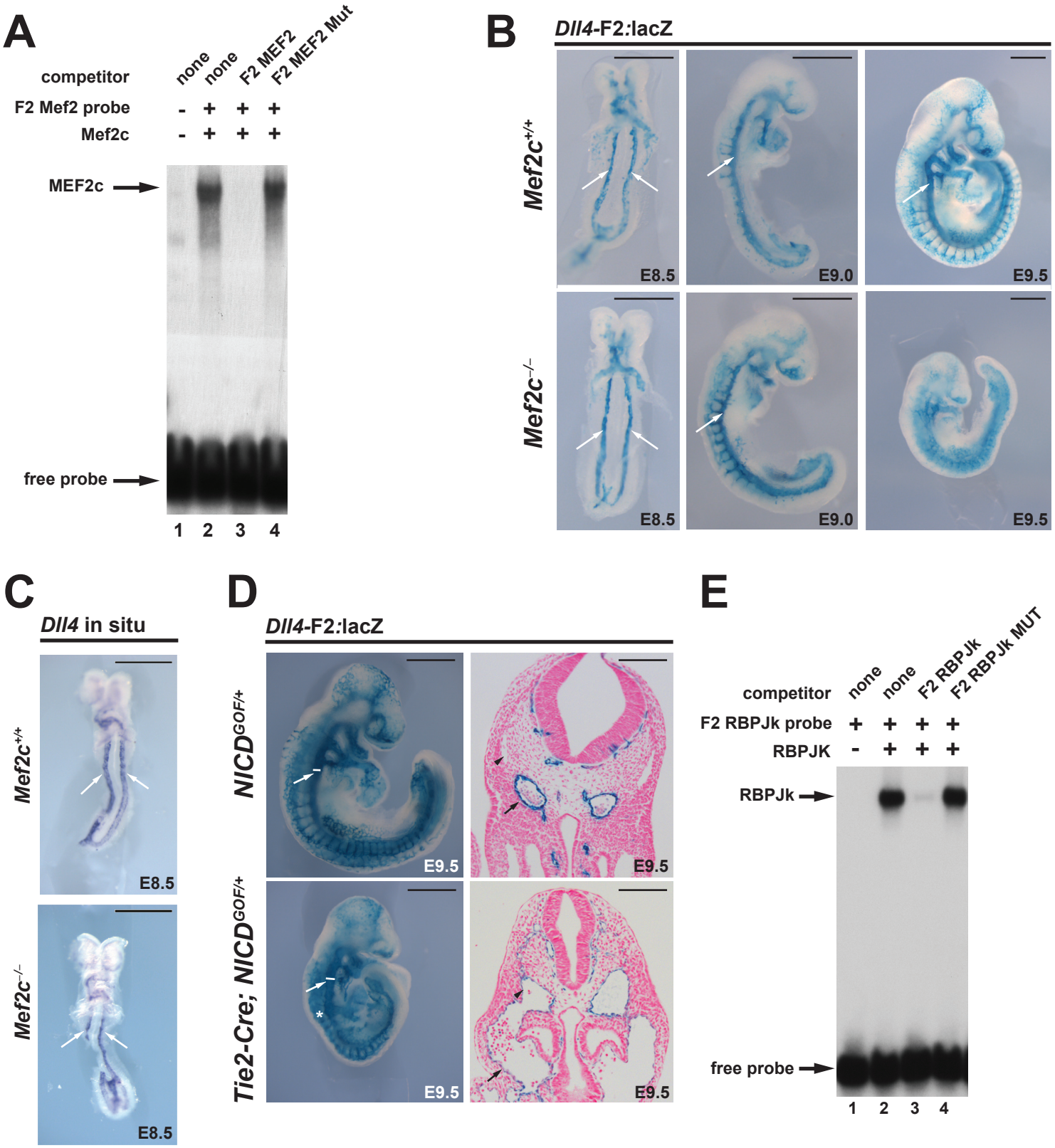

Wythe et al_Figure S2

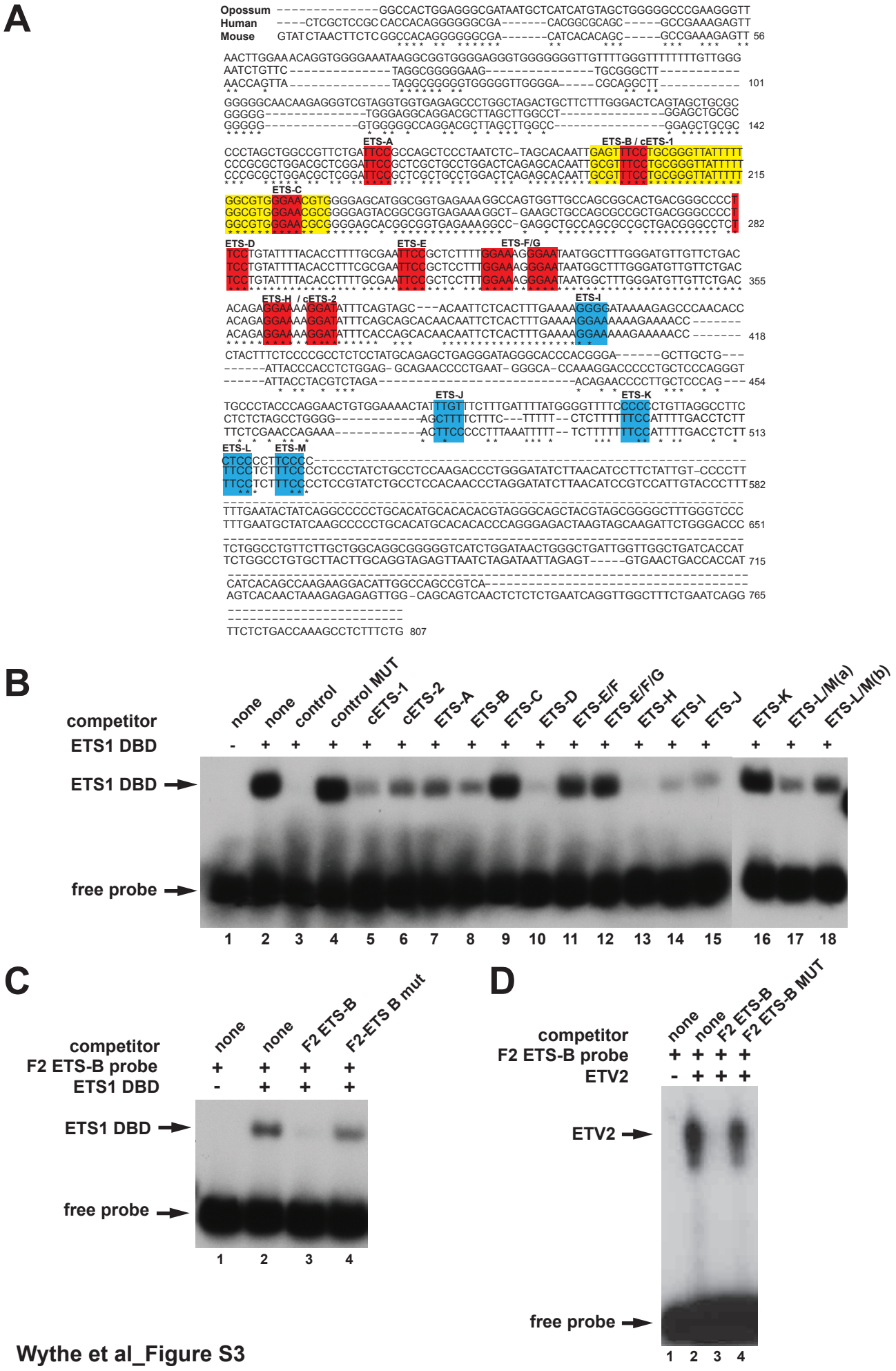

Wythe et al_Figure S3

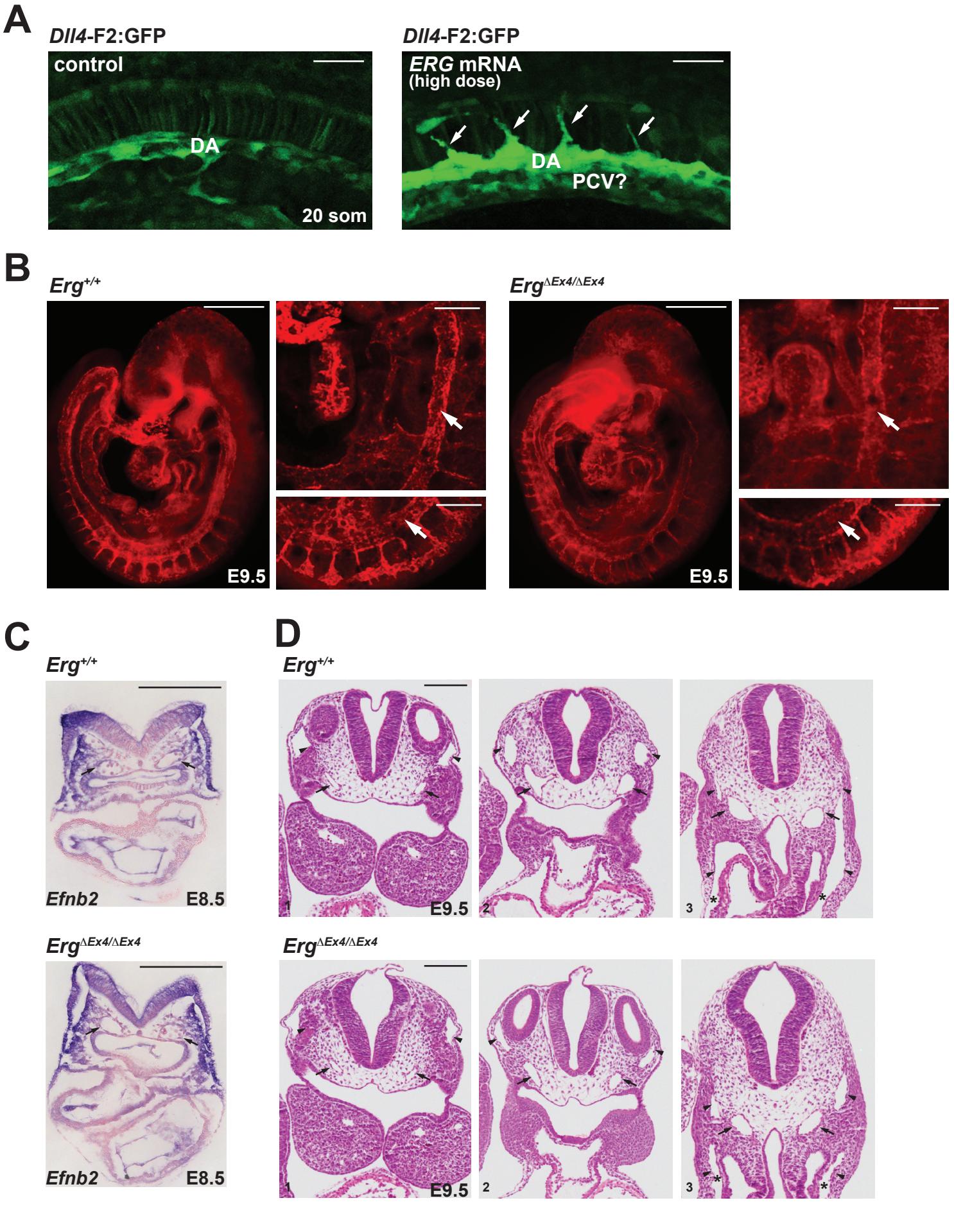

Wythe et al_Figure S4

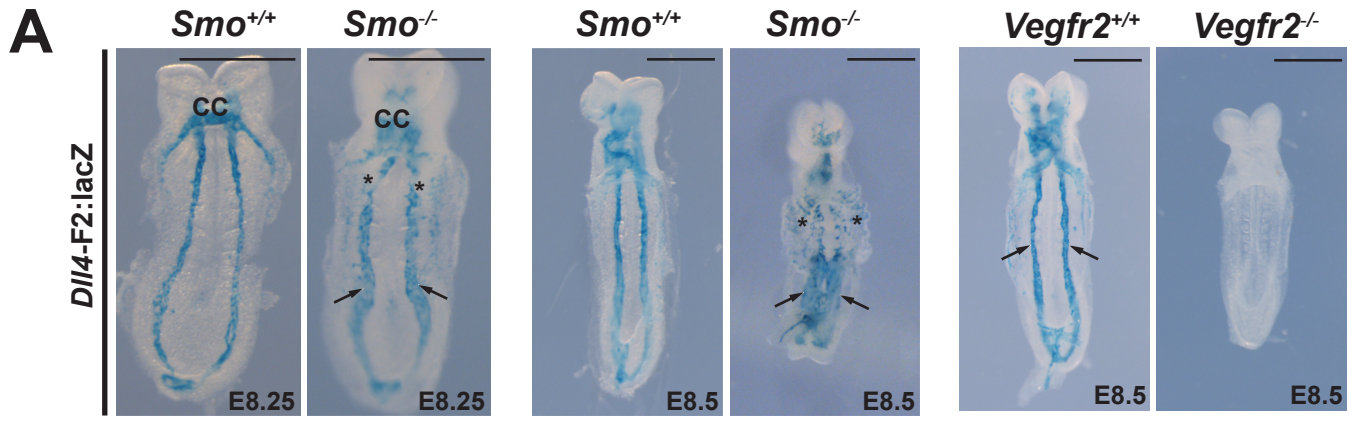

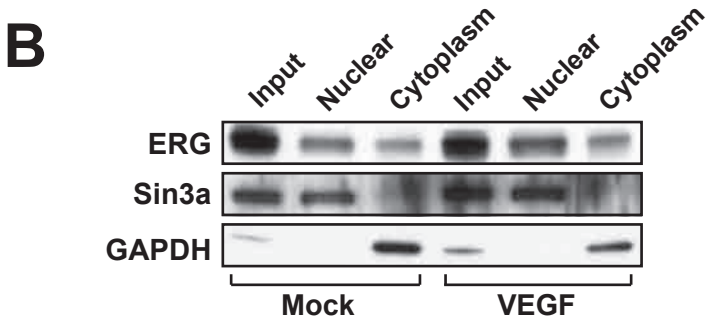

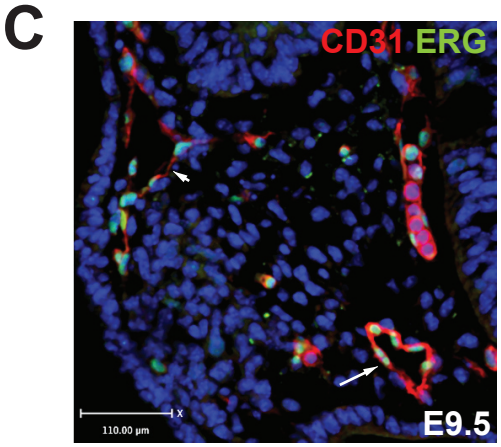

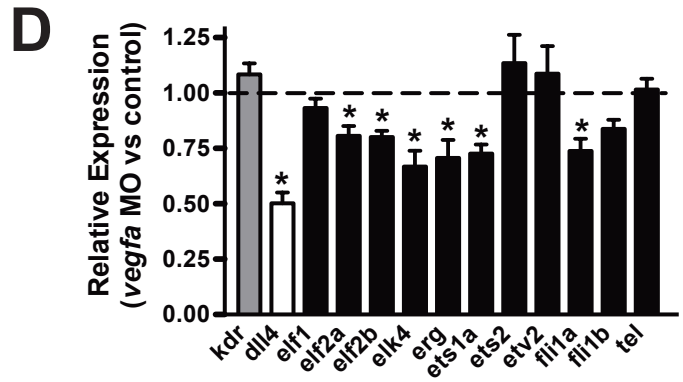

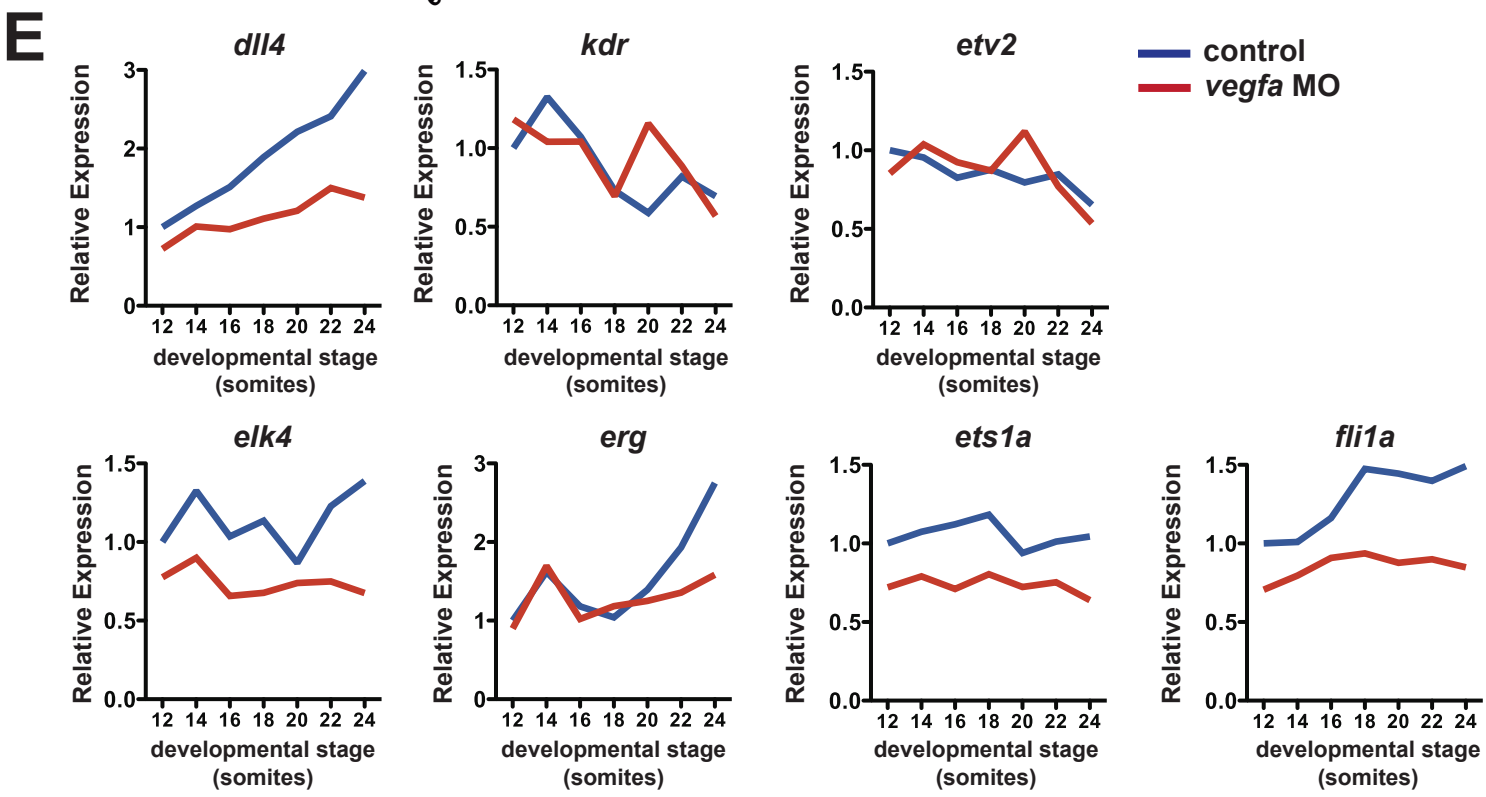

Wythe et al_Figure S5

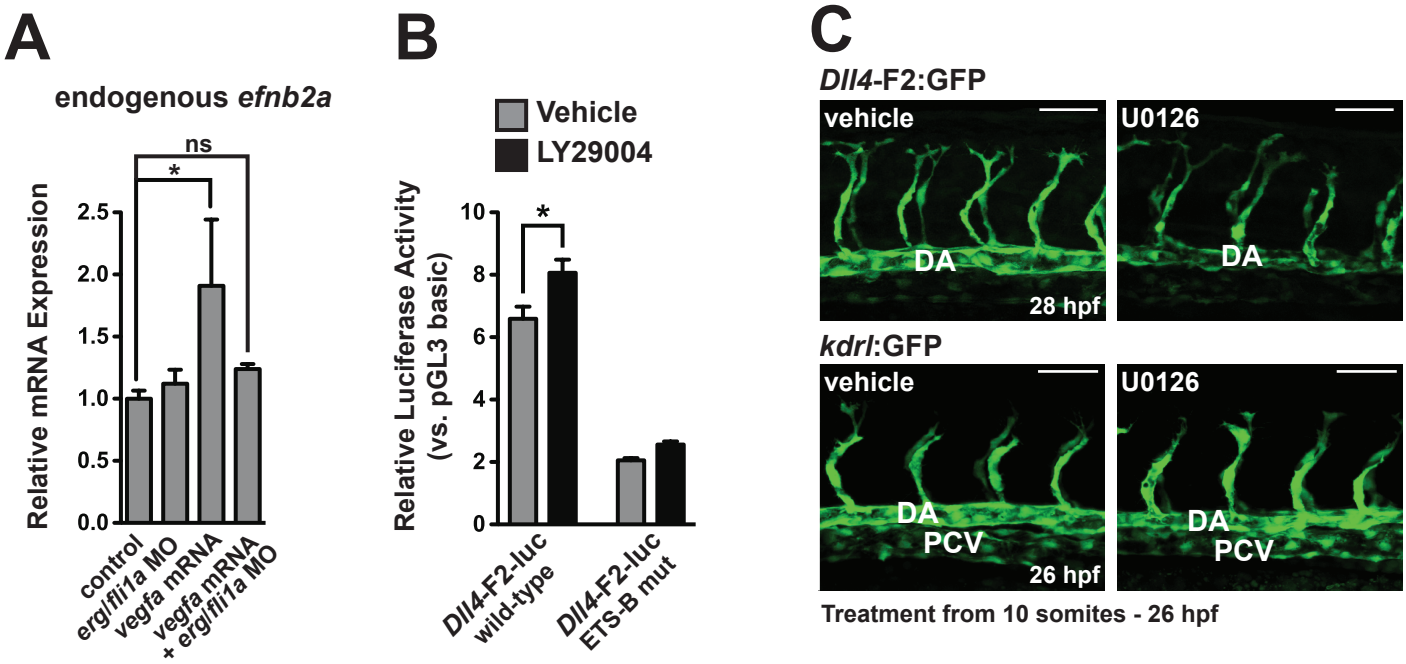

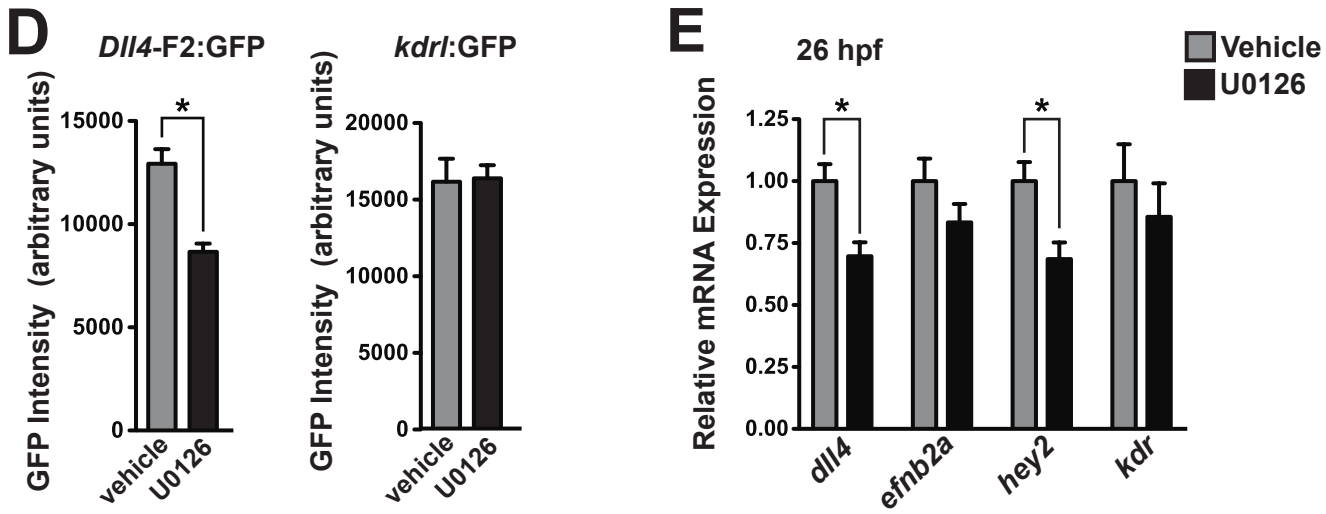

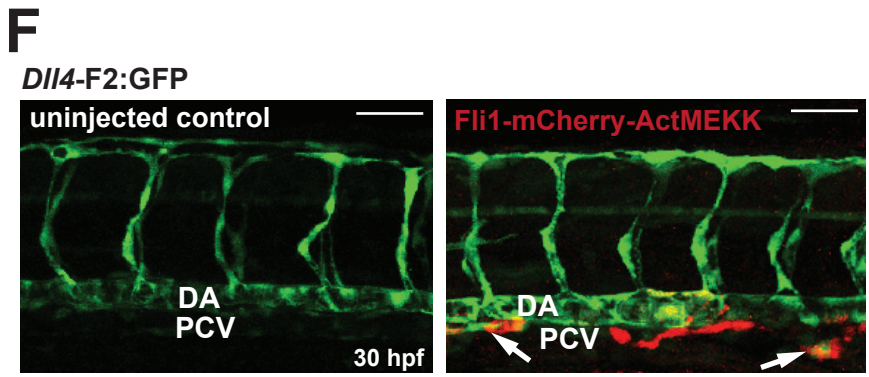

Wythe et al_Figure S6

Table S1 (Related to Experimental Procedures) - Primers used for qRT-PCR and ChIP analyses: Species of the gene and sequences of primers are indicated. Primers used for ChIP analyses are indicated as 'ChIP' primers.

Gene	Forward Primer 5'-3'	Reverse Primer 5'-3'
human *DLL4*	TGCGAGAAGAAAGTGGACAG	ACAGTAGGTGCCCGTGAATC
human *NOTCH4*	CTGGCTGTCCACCCTCAT	GAGCTGGAGGACGAGAAGAG
human *TBP*	TCGGAGAGTTCTGGGATTGT	CACGAAGTGCAATGGTCTTT
bovine *COUP-TFII*	CGGATCTTCCAAGAGCAAGT	TCAGAGAGACCACAGGCATC
bovine *DLL4*	GGCAATGCACTTGTGATGA	GGCGACAGGTGCAGGTAT
bovine *EFNB2*	CCAGACAAGAGCCATGAAGA	TGGTTTGACAAAGGGACTTG
bovine *EPHB4*	AGTGGCTTCGAGCCATTAAG	AGCAGGTCCTCAGTGGAGAT
bovine *HES1*	TGGAAATGACAGTGAAACACC	GTCACCTCGTTCATGCACTC
bovine *NOTCH1*	AACAACGTGGAGGCTGCT	ACCTTGGCGGTCTCGTAG
bovine *NOTCH4*	TGGTTGAAGAACTGATTGCAG	CATCCTGTGCGTCTTTATCG
bovine *TBP*	GGTTAGAAGGCCTTGTGCTT	GGAGAACAATTCTCGGTTTGA
zebrafish *dll4*	GGACAAATGCACCAGTATGC	GTTTGCGCAGTCGTTAATGT
zebrafish *efnb2a*	CAGTTACCCTCCCAAACACC	CTCCCTTATCTTCCCCATGA
zebrafish *elf1*	CTTCTGCAGACGGTTCATGT	GTCATTGGACCTCCTCCTTG
zebrafish *elf2a*	CCTCAGGACAAGATGCCTTT	TTCTGACCCTGTGTCGTCAT
zebrafish *elf2b*	GTTCAGCGCACAGTAATGGT	ACCGTGGAGATCTTCTGTCC
zebrafish *elk4*	ATTTCTGGAGCACGCTGAG	TGTGTTGGTGCCGTCTAAAT
zebrafish *erg*	AGATTTTAGGGCCGACCAG	TGATGCAGGACGAGTTGC
zebrafish *ets1a*	AGCTCCAGCTTCCAGGAGT	TATTCAGACGGAGGGACACA
zebrafish *ets2*	CCACCTGTCAGAGCATCATC	TCTTGGGCTTGTTCTTCCTC
zebrafish *etv2*	CCTGCTTTGCTGCTCTGCTTC ATAC	TCCCACAATGGACACCAGCAGC
zebrafish *fli1a*	TGACGACCAATGAGAGGAGA	CGTGTCGATCTCCTGAAGAC
zebrafish *fli1b*	CCAAGCATTAGGTTCCATCA	TCGGAAAGCAACTCCAGTAA
zebfafish *kdr*	CTCACCTTCAACGTGGCTAA	TGATGTTCAAGGTTGGAGGA
zebrafish *kdrl*	AAGGCTTCTTCACTCTTCACG	GAGTGTGAGTGTCCCACCAA
zebrafish *tel* (*etv6*)	CACGAGCGCTCAGACACTAC	CTGACTCCAGATGCTCCAGA
zebrafish *tbp*	TGGGTTTCCCTGCCAAATTCTT	GGAAATAACTCCGGTTCATAGCTGC
human/bovine *DLL4* intron 3 (F2) ChIP	GTTTCCTGCGGGTTATTTTT	CTTTCCAAAGGAGCGGAAT
human *DLL4* exon 11 ChIP	CCCATGCCTCCAACTACTGT	GGGTAGACGGACATTCTTGC
bovine *DLL4* exon 11 ChIP	GGAAATTCTGGTGAGGGAGA	GAAGATCGGCTTCAAGGGTA
bovine *NOTCH4* intron 1 ChIP	TGGAGACATGGGAAAGTCAA	GAGGTGAATGGCTGAAACAC

Table S2 (Related to Supplemental Experimental Procedures) - Primers used for genotyping analyses: The allele, mouse genome informatics (MGI) number, primer sequence and amplicon size for transgenic, wild-type (WT) and knock-out (del) alleles are indicated.

MGI #	Allele	Forward 5'-3'	Reverse 5'-3'	Band Size
3056400	$Dll4^{lacZ/+}$ WT allele	GGGGAATCAGCTTTTCAGGAA	CGAACTCCTGCAGCCGCAGCT	300 bp
	$Dll4^{lacZ/+}$ lacZ allele	GGGGAATCAGCTTTTCAGGAA	ACGACGTTGTAATACGAC	110 bp
	$Cttnb1^{fl/+}$ WT/flox	AAGGTAGAGTGATGAAAGTTGTT	CACCATGTCCTCTGTCTATTC	221 bp 324 bp
2148569	$Cttnb1^{fl/+}$ del allele	TACACTATTGAATCACAGGGACTT	CACCATGTCCTCTGTCTATTC	500 bp
	$Rbpjk^{fl/+}$ WT allele	ACCAGAATCTGTTTGTTATTTGCATTACTG	ATGTACATTTTGTACTCACAGAGATGGATG	300 bp
	$Rbpjk^{fl/+}$ del allele	ACCAGAATCTGTTTGTTATTTGCATTACTG	TCCACCATGATTTGCTTGAG	700 bp
3697064	BAT-gal	CATTTCCCCCAAAACACATC	GTTTTCCCAGTCACGACGTT	218 bp
3836891	Axin2-d2EGFP	TCAGATTTCGCTTTTGAAAAAGCTGCGTCG	TGTGGTCGGGGTAGCGGCTG	500 bp
3579503	$Axin2^{nlacZ/+}$ WTallele	AAGCTGCGTCGGATACTTGCGA	AGTCCATCTTCATTCCGCCTAGC	493 bp
	$Axin2^{nlacZ/+}$ lacZ allele	AAGCTGCGTCGGATACTTGCGA	TGGTAATGCTGCAGTGGCTTG	400 bp
3603182	$Mef2c^{-/+}$ WT allele	GTGATGACCCATATGGGATCTAGAAATCAAGGTCCAGGGTCAG	CTACTTGTCCCAAGAAAGGACAGGAAATGCAAAAATGAGGCA	586/838 bp
	$Mef2c^{-/+}$ del allele	GTGGGCTCTATGGCTTCTGAGGCGGAAAG	CTACTTGTCCCAAGAAAGGACAGGAAATGCAAAAATGAGGCA	253 bp
5443838	$Erg^{Ex4/+}$ del allele	TTGTTCCCACGGAGAATCCGA	TCATCGGTCAGACGATTCATTGGCA	949 bp
	$Erg^{Ex4/+}$ WT allele	CACCTCTGTGTGGGATTCCT	ATGATGGCCATTAAGGCTTG	542 bp
	Generic lacZ	GCCAAAATCACCGCCGTAAG	TCGCTGGGGAATGAATCAGG	320 bp
	F2/3/4-lacZ	ACGGGCCTCTTCCTGTATTT	AGTGCTGCCTCTGACCTCAT	400 bp
3810530	Tie2-Cre	CCCTGTGCTCAGACAGAAATGAGA	CGCATAACCAGTGAAACAGCATTGC	560 bp
2176255	$Smo^{del/+}$ WT allele	CACCGGTCGCCTAAGTAGC	CCAGCAGTACCAGCAGCAG	190 bp
	$Smo^{del/+}$ del allele	CACCGGTCGCCTAAGTAGC	GCCAGAGGCCACTTGTGTAG	240 bp
3629041	$Flk1^{GFP/+}$ WT allele	TGGAGAGCAAGGCGCTGCTAGC	CTTTCCACTCCTGCCTACCTAG	322 bp
	$Flk1^{GFP/+}$ GFP allele	CCCCCTGAACCTGAAACATA	CTTTCCACTCCTGCCTACCTAG	600 bp
2684314	$R26^{N1ICD}$ WT allele	CCAAAGTCGCTCTGAGTTGTTATC	GAGCGGGAGAAATGGATATG	604 bp
	$R26^{N1ICD}$ del allele	AAAGTCGCTCTGAGTTGTTAT	GAAAGACCGCGAAGAGTTTG	320 bp

Supplemental Figure Legends

Figure S1 (Related to Figure 1): Wnt/β-Catenin signaling is not active in early arteries and does not regulate early *Dll4* expression. (**A**) Conservation between murine and opossum *Dll4* with location of fragment 1 (F1) indicated. Transgenic analysis of F1-*lacZ* (E9.5) is below. (**B**) Representative whole-mount F1-*lacZ* transgenic embryo. (**C**) Whole-mount (left) and transverse sections (right) of *BAT-gal* embryos at E8.5 (n=5) and E9.5 (n=4). Dorsal aorta (arrow); cardinal vein (caret). (**D**) Whole-mount (left) and zoomed-in (right) *Axin2-d2EGFP* embryos at E8.5 (n=6) and E9.5 (n=8). (**E**) Whole-mount (left) and transverse sections (right) of $Axin2^{nlacZ/+}$ embryos at E8.5 (n=3) and E9.5 (n=5). (**F**) Vascular patterning in endothelial-specific *β-catenin* loss-of-function (ECKO) embryos was normal, as visualized by Cre-mediated recombination of a GFP reporter allele (*Rosa26-mTomato-lox-stop-lox-mGFP* [*mTmG*]) (left). The dorsal aorta (arrow) and cardinal vein (caret) are indicated. A zoomed-in view (right) of the brain vasculature demonstrates a less remodeled vascular plexus (indicated by arrows) in the ECKO (n=7) embryonic brain compared to control (n=10) embryos. (**G**) *Dll4* in situ hybridization indicates normal expression in the dorsal aorta (arrow) of β-*catenin* ECKO embryos (n=4). (**H**) No defects in arteriovenous morphology in β-*catenin* null (n=5) embryos were observed, as assessed by ink injection (as ink filled the entire dorsal aorta (arrows)) and H&E histology of serial cross-sections through the rostral and caudal planes of the dorsal aortae and cardinal veins. Dorsal aorta (arrow); cardinal vein (caret). Scale bars: 500 μm (B-H, whole-mount), 100 μm (C-H, sections and zoom ins).

Figure S2 (Related to Figure 3): MEF2C and RBPJk bind to the F2 enhancer, and over-expression of NICD in the endothelium can drive F2 expression in the vein, while MEF2C is dispensable for early arterial *Dll4* expression. (**A**) Recombinant MEF2C protein was used in an electrophoretic mobility shift assay (EMSA) with a radiolabelled double-stranded oligonucleotide representing the F2-6 MEF2 binding site. Lane 1 contains reticulocyte lysate without recombinant MEF2C (represented by a minus sign). MEF2C efficiently bound to the F2-6 MEF2 site (lane 2) and this binding was efficiently competed by an excess of the unlabeled wild type F2-6 MEF2 element (lane 3), but not by an excess of a mutant form of this site (lane 4). (**B**) The F2-*lacZ* enhancer was crossed into the $Mef2c^{+/-}$ background, and wild-type and homozygous mutant embryos were stained for X-gal at E8.5, 9.0, and E9.5. No difference in enhancer activity was observable in mutant embryos compared to wild-type ($Mef2c^{+/+}$) littermates at early stages of vascular development (i.e. E8.5-E9.0) ($n \geq 5$ for each genotype). The dorsal aorta is indicated by arrows. Scale bars = 500 μm (**C**) Expression of *Dll4* mRNA was examined by in situ hybridization in $Mef2c^{+/+}$ and $Mef2c^{-/-}$ embryos. No difference in expression was noted at E8.5 (n=3 for each genotype). Scale bars = 500 μm (**D**) NICD was over-expressed in the endothelium via Tie2-Cre-mediated activation of a $R26^{N1ICD}$ allele. Whole-mount images (left; scale bar = 500 μm) and sections (right; scale bar = 100 μm) are shown. The presence of an arteriovenous malformation (AVM) is indicated by an asterisk and the dorsal aorta (arrow) and cardinal vein (caret) are also indicated. Expression of F2 was expanded into the cardinal vein in Notch over-expression embryos. (**E**) EMSA showing RBPJk binding to a probe corresponding to the F2-6 RBPJk site. Binding was competed by an excess of unlabeled wild-type but not RBPJk mutant probe.

Figure S3 (Related to Figure 4): The *Dll4* F2 enhancer contains multiple ETS binding sites. (**A**) ClustalW analysis of the 802-bp *Dll4* F2 evolutionarily conserved region (ECR), comparing mouse, human, and opossum sequences. The region contains 9 perfectly

conserved ETS consensus (GGA(A/T)) sequences (red boxes). Murine F2 contains a total of 14 ETS sites, with five more non-conserved sites (blue boxes). The minimal 36-bp enhancer (F2-6) is highlighted (yellow box). Asterisks denote conserved nucleotides across all three species. (**B**) Recombinant ETS1 DNA-binding domain (DBD) was used in EMSA with radiolabelled probe encompassing a confirmed ETS-binding site from the *Mef2c* F7 enhancer. Lane 1 contains reticulocyte lysate lacking ETS1 DBD. ETS1 DBD bound the bona fide ETS-binding site in the control probe (*Mef2c* F7) (lane 2) and this specific binding was competed away by unlabeled control probe (lane 3), but binding was not competed by a control probe with a mutated ETS site (lane 4). Unlabeled probes corresponding to each of the potential ETS sites in the *Dll4* F2 enhancer were used as competitors for ETS1 DBD binding to the control probe (lanes 5-18). The *Dll4* F2 sites competed for ETS DBD binding to varying degrees. Probes encompassing ETS-B, ETS-D, ETS-H, ETS-I, ETS-J, and ETS-L competed most efficiently (lanes 8, 10, 13, 14, 15, 17, respectively). In addition to the GGA(A/T) core, ETS-B and ETS-H possessed (or overlapped with) canonical ETS sites (cETS). cETS-1/ETS-B was a consistent competitor (lanes 5 and 8), and directly bound the ETS1-DBD (panel C), but cETS-2 (lane 6) and ETS-H (lane 13) did not compete consistently, and they did not bind the ETS1-DBD directly (data not shown). (**C**) EMSA showing binding of ETS1 DNA binding domain (DBD) to the ETS-B site of F2-6. Binding was competed by an excess of unlabeled wild-type but not ETS-B mutant probe**.** (**D**) EMSA was performed using F2 probe and recombinant ETV2 protein. Wild-type F2 sequence effectively competed for ETV2 binding, but this competition was lost when the ETS-B site was mutated.

Figure S4 (Related to Figure 4): Analysis of ERG gain- and loss-of-function phenotypes. (**A**) Injection of high doses of *ERG* mRNA (400 pg) in zebrafish embryos resulted in enhanced F2:GFP expression at the 20-somite stage. Premature sprouting of intersomitic vessels (arrows) was also observed. Cells were present ventral to the dorsal aorta that express F2:GFP. These may be ventrally sprouting posterior cardinal vein cells. Scale bar = 50 μm. (**B**) Wild-type (n=2) and $Erg^{\Delta Ex4/\Delta Ex4}$ (n=2) embryos (E9.5) were stained with PECAM antibodies and confocal microscopy was utilized to observe vascular patterning. The dorsal aorta (arrow) was present and morphologically normal in *Erg* knock-out embryos. Scale bars = 500 μm (wholemount) and 110 μm (zoom ins). (**C**) Section in situ hybridization at E8.5 reveals reduced *Efnb2* mRNA in the dorsal aorta (arrows) in *Erg* knock out embryos (n=2) compared to wild-type littermates (n=2). Sections are counter-stained with nuclear fast red. Scale bar = 100 μm. (**D**) Histology of serial cross-sections through wild-type (n=3) and *Erg* knock-out embryos (E9.5) (n=2) did not reveal gross morphological defects in arteries or veins. Dorsal aorta (arrow); cardinal vein (caret). Scale bar = 100 μm.

Figure S5 (Related to Figure 5): Regulation of F2 enhancer activity by Vegf in mouse embryos and regulation of ETS factors by Vegf at early stages of zebrafish embryogenesis. (**A**) F2-lacZ expression in the anterior DA (asterisk) is reduced in *Smoothened*$^{-/-}$ *(Smo)* embryos ($Smo^{+/+}$, n=10; $Smo^{-/-}$, n=3) at E8.25 and absent by E8.5 ($Smo^{+/+}$, n=8; $Smo^{-/-}$, n=4). CC, cardiac crescent. Dorsal aorta (arrows). F2 activity was abolished in $Vegfr2^{-/-}$ embryos ($Vegfr2^{+/+}$, n=12; $Vegfr2^{-/-}$, n=2). Scale bar = 500 μm. (**B**) Biochemical fractionation of untreated and VEGF-treated (20 minutes) BAEC was performed and localization of ERG was analyzed. Sin3a and GAPDH were utilized as markers for nuclear and cytoplasmic protein expression, respectively. No difference in ERG localization was observed upon VEGF treatment. (**C**) Immunofluorescence of E9.5 mouse embryonic tissue for ERG (green) shows that endothelial cells, marked by

PECAM/CD31 (red), in the dorsal aorta (arrow) have stronger nuclear (DAPI) ERG expression and are more often expressing ERG than the vein (caret). Scale bar = 110 μm. (**D**) Various ETS factors that are enriched in expression in endothelial cells (black bars) and *dll4* (white bar) were measured by qRT-PCR in control or *vegfa* morpholino-injected embryos at the 20-somite stage. *kdr* expression (gray bar) was used to assess the amount of endothelium. Data is presented as expression in *vegfa* morphants compared to control embryos (n=3; mean ± SEM). * indicates a significant difference in expression between *vegfa* morphants and controls. (**E**) Detailed assessment of expression kinetics (qRT-PCR) were performed in control and *vegfa* morphants. A representative experiment is shown. *kdr* and *etv2* expression was not altered by knock-down of *vegfa*, while *elk4, ets1a, erg* and *fli1a* were down-regulated in *vegfa* morphants.

Figure S6 (Related to Figure 6 and Figure 7): The F2 enhancer and endogenous *Dll4* expression are regulated by Vegf/MAP kinase signaling. (**A**) From the experiment shown in Figure 6C,D, induction of Vegfa-inducible *efnb2* was also inhibited in embryos injected with *erg/fli1a* morpholinos. Shown is qRT-PCR from 5 individual embryos per group (mean ± SEM). * indicates a significant difference by 1-way ANOVA. ns, not significant. (**B**) F2-luciferase activity was enhanced upon inhibition of PI3 kinase signaling (LY29004 treatment) in BAEC. The activity of F2-luciferase was decreased, and the responsiveness to PI3K inhibition was lost, when the *ETS-B* site was mutated. Shown is a representative experiment, triplicate determinations (mean ± SEM). (**C**) F2:*GFP* or *kdrl:GFP* embyros were treated the MAP kinase inhibitor, U0126, starting at the 10-somite stage, and imaging was performed at 26 or 28 hpf. F2:GFP expression was decreased in the presence of U0126, but *kdrl*:GFP was unaffected. (**D**) Quantification of (C) is shown (n=4 per group; mean ± SEM). (**E**) Expression of endogenous *dll4*, *efnb2a, hey2* and *kdr* was assessed by qRT-PCR (n=5-10 individual embryos; mean ± SEM). (**F**) Embryos were injected with a construct that drives expression of constitutively active MEKK in the endothelium (Fli1-mCherry-ActMEKK). In embryos with expression of the construct in the vein, F2:GFP expression was also observed in venous cells (arrows).

Supplemental Experimental Procedures:

Bioinformatic analyses, cloning, and mutagenesis

Mouse, human, and opossum sequences were compared using BLAST (Altschul et al., 1990) and VISTA (Mayor et al., 2000). The *Dll4* F1 fragment spanned 5,135 bp upstream of the GGG preceding the start codon in exon 1 (Chr2:119321006-119326140) and was cloned by PCR from a BAC (bMQ 132j23) containing mouse *Dll4*: forward, 5'-GGATCCTGTTGCTGCAGGCCCTAGACACTC, and reverse, 5'-GCGGCCGCCCCTTG GGGTGTCCTCTCCACTCC. A BamHI site was added to the forward primer and a NotI site was added to the reverse primer. The PCR fragment was purified, and cloned into Topo-XL. Upon verification by DNA sequencing, the insert was subcloned, via BamHI and NotI, into pENTR1a.

The 802-bp *Dll4* F2[1–802] fragment (Chr2:119327120-119327921) was generated by PCR using the following forward and reverse primers: 5'-ATCGGGGGATCCAGTATCTAACTTCTCGGCCACAGG-3′, and 5′ATCCGCGGCCGCGCAGAAAGAGGCTTTGGTCAGAGA-3′. The underlined sequences are homologous to murine *Dll4*. The primers contained BamHI and NotI on the forward and reverse primers, respectively, and were sub-cloned into pENTR1a (Invitrogen). *Dll4*-F2-pENTR1a was digested with EcoRI and NotI, deleting an internal fragment of 504 bp, and the remaining 2,580 bp plasmid was gel extracted, blunt-end filled, and ligated to itself and transformed to generate the F2-2 plasmid. The F2-3 fragment was constructed by digesting F2-pENTR1a with BamHI and EcoRI, releasing a 304 bp fragment. The 2,780 bp backbone was gel extracted, blunt-end filled, and ligated to itself and transformed. F2-4 was amplified from a BAC containing the *Dll4* locus by PCR using the following primers: 5'-ATCGGGGGATCCGCACAATTGCGTTTCCT GCGGG and 5'-ATCCGCGGCCGCGGTTTTTCTTTTTCCTTTTCAAGTGAG and cloned into pENTR1A via BamHI and NotI.

F2-6(3X) was directly synthesized (IDT) with 36-bp of *Dll4* repeated in triplicate (underlined), flanked 5' by attB1 and BamHI and 3' by NotI and attB2. F2-6(3X): 5'-ACAAGTTTGTACAAAAAAGCAGGCTGGATCCGCGTTTCCTGCGGGTTATTTT TGGCGTGGGAACGCGGCGTTTCCTGCGGGTTATTTTTGGCGTGGGAACGCG GCGTTTCCTGCGGGTTATTTTTGGCGTGGGAACGCGGCGGCCGC CCCAGCTTTCTTGTACAAAGTGGT-3'. This was annealed, and duplexed DNA was recombined into pDonor-221 by a BP reaction to generate *Dll4*-F2-6(3X)-p221 for subsequent LR reactions.

The deletion construct *Dll4*-F2Δ2 [Δ1482-1518] was generated by a 3-way Cold Fusion (SSI) ligation of linearized pENTR1a with two purified PCR products flanking the 5' and 3' ends of a 36-bp core in F2 (deleting the ETS, MEF2, RBPJk, and E2F sites). The 5' flanking fragment was amplified using the following primers: 5′-AACCAATTCAGTCGACTGAGTATCTAACTTCTCGGCCACAGG (homology to pENTR1a underlined), 5'-GGATCCGCGGCCGCGGATCCAATTGTGCTCTGAGTC CAGGCAGC (polylinker underlined). The 3' half of F2Δ2 was amplified using primers: 5' GGATCCGCGGCCGCGGATCCGGGAGCGCGGCGGTGAGAAAGG (linker homology underlined) and 5'- GGTCTAGATATCTCGAGTGCGGCCGCAGAAAGAGGCTTTGG TCAGAGA (pENTR1a homology underlined). PCR replaced the 36-bp core with an internal BamHI-NotI-BamHI polylinker. After confirmation by sequencing, the intervening sequence between the 5' and 3' fragments was removed by digestion with BamHI, the backbone was purified and ligated to generate F2Δ2. F2Δ2 was digested with BamHI and EcoRI, end-filled, and the backbone purified and ligated to generate F2Δ1 [Δ1482-

1598]. F2Δ2 was digested with BamHI and NotI, end-filled, and the purified backbone ligated to itself to generate F2-5 pENTR1a.

To generate mutant constructs, the desired mutations validated by EMSA (see below) were engineered into either F2-6(3X)-pDONR-221 or F2-pDONR-221. For F2-6(3X), ultramer oligos with the desired mutation were synthesized (IDT), just as for wild-type F2-6(3X), annealed, and duplexed DNA was recombined into pDONR-221 via a BP reaction. Plasmids with the desired transcription factor binding mutation within F2 were directly synthesized (IDT). The inserts were then amplified from the synthetic plasmids by PCR with attb1 and attb2 sequences in the 5' and 3' oligos, respectively (5'-ACAAGTTTGTACAAAAAAGCAGGCTGGATCCAGTATCTAACTTCTCGG CCACAGG; 5'- ACCACTTTGTACAAGAAAGCTGGGGCGGCCGCAGAAAGAGGCTTTGGTCA GAGA) (homology to *Dll4* F2 is underlined). These inserts were purified, and recombined into pDONR-221 via a BP reaction, and sequenced to confirm the mutation. All mutant clones were then shuttled into pGL3pro-DV (a modified version of pGL3-promoter-luciferase containing a Gateway Destination Vector), tol2-E1b-GFP, and *hsp68-lacZ* destination vectors by LR recombination reactions.

Generation of transgenic mice

The pBSK-AUG-β-gal plasmid was digested in the polylinker using a blunt-cutter (SmaI) and an RFA "B" Gateway cassette (Invitrogen) was inserted 5' to the promoterless AUG-*lacZ* reporter to make a destination vector (pBSK-*AUG-lacZ*-DV). A similar strategy was used to modify pBSK-*hsp68-lacZ* (Kothary et al., 1989), to obtain pBSK-*hsp68-lacZ*-DV. Upon LR recombination with DONR or entry clones and destination reporter plasmids, the final vectors were restriction mapped and verified by DNA sequencing. Transgenic *lacZ* reporter fragments were generated by gel purifying SalI fragments from recombined *AUG-lacZ*-DV or hsp68-*lacZ-DV* plasmids. Pronuclear injection of transgenic fragments was performed at the Gladstone Institute, or by Cyagen Biosciences (Gunzu, China). The presence of *lacZ* transgenes in embryo yolks sacs was detected by PCR using primers specific for the transgene, or for *lacZ* (5'-TCGTTGTGCATAAACCGACT; 5'-GACCATTTTCAATCCGCACCT). All experiments using mice were reviewed and approved by the UCSF Institutional Animal Care and Use Committee and complied with all institutional and federal guidelines.

Genotyping and mice used

$Dll4^{lacZ/+}$ ($Dll4^{tmJrt}$) (Duarte et al., 2004) cryopreserved embryos were purchased from the Canadian Mouse Mutant Repository (CMMR) and implanted into CD31 females. *β-catenin* (*Cttnb1)* (Brault et al., 2001), *Axin2-d2EGFP* (Jho et al., 2002), *BAT-gal* (Maretto et al., 2003), $Axin2^{lacZ/+}$ (Lustig et al., 2002), *Rbpjk* (Han et al., 2002), *Erg* (Vijayaraj et al., 2012), *Mef2c* (Vong et al., 2005), *Smo* (Zhang XM et al., 2001),*Vegfr2* (Ema et al., 2006), $R26^{N1ICD}$ (Murtaugh et al., 2003), and *Tie2-cre* (Braren et al., 2006) mice have all been described previously. $Mef2c^{flox/+}$, $Cttnb1^{flox/+}$ and $Rbpjk^{flox/+}$ mice were each mated to *Mef2c*-AHF-Cre females (which acts as a universal deleter strain in the female germ line) to generate offspring with global null (deleted, or del) alleles. Matings were designed so that only one LoxP-flanked (floxed) allele needs to undergo recombination to create endothelial-specific knockout mice. In the first cross, heterozygous del mice were bred to a *Tie2-Cre* transgenic male (to avoid female germ line activity of *Tie2-Cre*) (de Lange et al., 2008), and the resulting male offspring that inherited the del allele and *Tie2-Cre* transgene were then mated to females homozygous for the floxed allele to generate endothelial-specific loss-of-function (ECKO) embryos. All floxed alleles were maintained in a $R26^{mTmG/mTmG}$ (Muzumdar et al., 2007) background. Endothelial-specific activity of *Tie2-Cre* was confirmed by GFP immunofluorescence within the endothelium.

Where appropriate, the *F2-hsp68-lacZ* transgene was maintained in males. Genotyping for all alleles was performed by PCR (see Table S2 for primer sequences).

Electrophoretic mobility shift assay (EMSA)

EMSA was performed as before (Dodou et al., 2003). Briefly, double-stranded oligonucleotides containing 5' and 3' GG overhangs were labeled with ^{32}P-dCTP, using Klenow to fill in overhanging 5' ends, and purified on a non-denaturing polyacrylamide-TBE gel. Binding reactions were pre-incubated at room temperature in modified 1x binding buffer (15 mM KCl, 5 mM Hepes pH 7.9, 5% glycerol, 0.04 mM EDTA, 0.125 mM DTT, 0.25 mM PMSF) containing recombinant protein, 1 ug of poly dI-dC, and unlabeled competitor DNA (50-fold excess, where indicated) for 10 min before probe addition. Reactions were incubated an additional 20 min at room temperature after probe addition and electrophoresed on a 10% nondenaturing polyacrylamide gel.

The DNA-binding domain of murine ETS-1 in pCITE-2A (Novagen) containing the 85 amino acids ETS domain but no auto-inhibitory domain, efficiently binds *bona fide* ETS sites (Nye et al., 1992), and has been described before (De Val et al., 2004). The full-length ETV2-pCITE-2A (De Val et al., 2008) and pCDNA3.1-RBPJk (Liang et al., 2002) have been described before, and the pCITE-2B-MEF2C cloning will be detailed elsewhere. All recombinant proteins were transcribed and translated using the TNT Coupled Transcription–Translation system (Promega) according to the manufacturer's instructions.

The ETS1 control (*Mef2c*-F7 ETS-A) and mutant control probe sequences have been described previously (De Val et al., 2004) and were: control, 5′-gctcagagaaggaagtggagagt-3′; mutant, 5′-gctcagagaag**ctt**gtgggaggtt-3′. The sequences of the competitor oligonucleotides encompassing the ETS sites from the *Dll4* F2 enhancer were:

1) ETS-A, 5′-GGTGGACGCTCGGATTCCGCTCGCTGCCTG-3'.
2) ETS-B/cETS-1a site, 5′-GGGCACAATTGCGTTTCCTGCGGGTTATTT-3';
3) ETS-C, 5′-GGATTTTTGGCGTGGGAACGCGGGGAGCGC-3';
4) ETS-D, 5′-GGCTGACGGGCCTCTTCCTGTATTTTACAC-3';
5) ETS-E(/F), 5′-GGACCTTTTGCGAATTCCGCTCCTTTGGAAA-3';
6) ETS-E/F/G, 5′-GGTTCCGCTCCTTTGGAAAGGGAATAATGG-3';
7) ETS-H /cETS-1b site, 5′-GGTTCTGACACAGAGGAAAAGGATATTTCA-3';
8) ETS-I (NFATc1), 5′-GGTCACTTTGAAAAGGAAAAAGAAAAACCA-3′;
9) ETS-J, 5′-GGGAACCAGAAAACTTCCCCCTTTAAATTT-3′;
10) ETS-K, 5′-GGTTTTTTCTTTTTTTCCATTTTGACCTCT-3';
11) ETS-L/M-#1, 5′-GGTTTTGACCTCTTTTCCTCTTTCCCCTCC-3';
12) ETS-L/M-#2, 5′-GGCTCTTTTCCTCTTTCCCCTCCGTATCTG

cETS-1b, 5' GGTCTGACACAGAGGAAAAGGATATTTCACCAGCACAAC

cETS-1a, 5' GGCAGAGCACAATTGCGTTTCCTGCGGGTTATTTTTGGCG

cETS-1a mut, 5' GGCAGAGCACAATTGCGTTT**tt**TGCGGGTTATTTTTGGCG

The sequences for the ETS mutant sites were identical to the mutagenic primers described above. For the ETS-6X mutant, ETS sites B, D, H, I, J, and L were all mutated in cis as described above.

The sequences of the RBPJk sites within *Dll4* F2 were: *Dll4* F2 RBPJk, 5′-GGGGTTATTTTTGGCGTGGGAACGCGGGGAGCGC-3′; *Dll4* F2 RPBJk Mutant, 5′-GGGGTTATTTTTGGC***aaccct***ACGCGGGGAGCGC-3′. The sequences of the MEF2 sites within *Dll4* F2 were: *Dll4* F2 MEF2, 5′-GGATTGCGTTTCCTGCGGGTTATTT TTGGCGTGGGAACGCGGGGAGCG-3′. Dll4 F2 MEF2 mutant, 5′-GGATTGCGTTTC CTGCGGGTTA**tggc**TGGCGTGGGAACGCGGGGAGCG.

Cloning of pCS2-V5-ERG
Human ERG open reading frame (ORF) was amplified from plasmid DNA (IMAGE clone #6052140) and a XhoI site, kozak sequence, and V5 epitope tag were added to the 5' end, while an XbaI restriction site was added to the 3' end (5'-ATCCCTCGAGGCCAC CATGGGTAAGCCTATCCCTAACCCTCTCCTCGGTCTCGATTCTACGATGGCCAGCA CTATTAAGGAAGC; 5'-GAATTCTAGATTATTAGTAGTAAGTGCCCAGATGAGAAGGC) and cloned into pCRII-TOPO-zero blunt. The insert was then subcloned into the pCS2 expression vector using XhoI and XbaI.

In situ *hybridization*
The murine *Dll4* riboprobe was from Janet Rossant (Duarte et al., 2004), and the *Efnb2* riboprobe, spanning the second to fifth exon of the *Efnb2* cDNA, was from Jeffrey Bush and Ace Lewis (UCSF). Embryos were processed as previously described (Wythe et al., 2011). CD31 immunostained embryos were embedded in 1% low melt agarose in PBS, and cleared in *Clear*^{T2} (Kuwajima et al., 2013) prior to imaging. Wholemount lacZ and indirect immunofluorescent images were obtained using a Leica dissecting microscope and camera with the Leica LAS Montage extended focus function. Confocal images were obtained on a Nikon ECLIPSE Ti 2000 confocal microscope with a Yokogawa CSU-X1 spinning disk and Hamamatsu ImagEM CCD camera. Images were processed using Velocity software (Perkin Elmer).

Zebrafish experiments
The *Tg(Dll4-F2-E1b:GFP)* line was generated by injecting a Tol2 construct containing the mouse *Dll4* F2 sequence (see below for details) into 1-cell embryos. Morpholinos against *vegfa* (5'-CTC GTC TTA TTT CCG TGA CTG TTT T (Ober et al., 2004), 2.5 ng), *rbpjk* (5'-CAA ACT TCC CTG TCA CAA CAG GCG C (Siekmann and Lawson, 2007), 2.5 ng), *erg* (5'-AGA CGC CGT CAT CTG CAC GCT CAG A, 8 ng) and *fli1a* (5'-TTT CCG CAA TTT TCA GTG GAG CCC G (Liu and Patient, 2008), 2ng) were injected into 1-2 cell embryos. For MAPK inhibition studies, embryos were dechorionated and treated with 20 μM U0126 (Invivogen) or DMSO from the 10-somite stage to 28 hpf. Vibratome sectioning, embedding of live and fixed embryos, and confocal analyses were performed as before (Fish et al., 2011). In some experiments indirect immunofluorescence of Tg(*Dll4*-F2:GFP) was performed as described previously (Fish et al., 2011). Quantification of GFP intensity was performed using ImageJ. For transgenesis experiments, enhancer elements were subcloned into pDONR 221 (Invitrogen), then recombined into a Destination Vector (Invitrogen) containing two tol2 sites flanking a gateway recombination site and a minimal promoter (E1b) driving EGFP (Birnbaum et al., 2012). 25-40 pg of Tol2-containing DNA plasmids and 35-75 pg of transposase mRNA were injected into the cell of 1-cell stage embryos. pCS2-mCherry, pCS2-transposase, pCMV-Sport6-ERG, pCS2-Vegfa121 and pCS2-Vegfa165 (both from Nathan Lawson) (Lawson et al., Dev Cell, 2002) were linearized and capped mRNA was transcribed using the SP6 mMessage mMachine Kit (Ambion). 200 pg or 400 pg of *ERG* mRNA were injected for rescue or phenotypic analyses, respectively. 300 pg of *Vegfa121* and 100 pg of *Vegfa165* were injected together. When *Vegfa121/165* mRNA and *erg/fli1a* morpholinos were injected in combination, 4 ng of *erg* morpholino and 1 ng of *fli1a* morpholino were used. In some experiments, 100 pg of *mCherry* mRNA was co-injected to determine which embryos were successfully injected with Tol2 constructs, or as a control mRNA. 100 pg of pTol-*fliepcherryactMEKK* (Covassin et al., 2009), which drives endothelial-specific expression of mCherry and constitutively-active mitogen activated protein kinase 1 (MAP2K1) (a kind gift of Nathan Lawson), was co-injected with transposase mRNA.

Quantitative reverse-transcriptase PCR (qRT-PCR)
RNA was isolated from cultured cells or pooled zebrafish embryos using Trizol (Invitrogen). RNA from individual zebrafish embryos was isolated using RNeasy Mini Kit (Qiagen). Mouse embryos were snap frozen and RNA was isolated using the RNAqueous Micro Kit (Ambion). RNA was reverse transcribed using the high-capacity cDNA reverse transcription kit (Applied Biosystems). qRT-PCR was performed using a Roche Lightcycler 480® with LC 480 SYBR Green I Master Mix (Roche) or LC 480 Probes Master Mix (Roche). Data were normalized to Tata box binding protein (*TBP*) or to *Gapdh* (mouse experiments) using the Delta-Delta Ct method. Sybr green primers are listed in Table S1. The following Assay On Demand probes were used for mouse genes: *Pecam1* (Mm01242576_m1), *Dll4* (Mm00444619_m1), *Notch1* (Mm00435249_m1), *Notch4* (Mm00440525_m1), *Cxcr4* (Mm01292123_m1), *Efnb2* (Mm01215897_m1), and *Gapdh* (4352932) (Applied Biosystems).

Supplemental References

Altschul, S.F., Gish, W., Miller, W., Myers, E.W., and Lipman, D.J. (1990). Basic local alignment search tool. J Mol Biol *215*, 403-410.

Birnbaum, R.Y., Clowney, E.J., Agamy, O., Kim, M.J., Zhao, J., Yamanaka, T., Pappalardo, Z., Clarke, S.L., Wenger, A.M., Nguyen, L.*, et al.* (2012). Coding exons function as tissue-specific enhancers of nearby genes. Genome Res *22*, 1059-1068.

Braren, R., Hu, H., Kim, Y.H., Beggs, H.E., Reichardt, L.F., and Wang, R. (2006). Endothelial FAK is essential for vascular network stability, cell survival, and lamellipodial formation. The Journal of cell biology *172*, 151-162.

Brault, V., Moore, R., Kutsch, S., Ishibashi, M., Rowitch, D.H., McMahon, A.P., Sommer, L., Boussadia, O., and Kemler, R. (2001). Inactivation of the beta-catenin gene by Wnt1-Cre-mediated deletion results in dramatic brain malformation and failure of craniofacial development. Development *128*, 1253-1264.

Covassin, L.D., Siekmann, A.F., Kacergis, M.C., Laver, E., Moore, J.C., Villefranc, J.A., Weinstein, B.M., and Lawson, N.D. (2009). A genetic screen for vascular mutants in zebrafish reveals dynamic roles for Vegf/Plcg1 signaling during artery development. Dev Biol *329*, 212-226.

de Lange, W.J., Halabi, C.M., Beyer, A.M., and Sigmund, C.D. (2008). Germ line activation of the Tie2 and SMMHC promoters causes noncell-specific deletion of floxed alleles. Physiol Genomics *35*, 1-4.

De Val, S., Anderson, J.P., Heidt, A.B., Khiem, D., Xu, S.M., and Black, B.L. (2004). Mef2c is activated directly by Ets transcription factors through an evolutionarily conserved endothelial cell-specific enhancer. Developmental biology *275*, 424-434.

De Val, S., Chi, N.C., Meadows, S.M., Minovitsky, S., Anderson, J.P., Harris, I.S., Ehlers, M.L., Agarwal, P., Visel, A., Xu, S.M.*, et al.* (2008). Combinatorial regulation of endothelial gene expression by ets and forkhead transcription factors. Cell *135*, 1053-1064.

Dodou, E., Xu, S.M., and Black, B.L. (2003). mef2c is activated directly by myogenic basic helix-loop-helix proteins during skeletal muscle development in vivo. Mech Dev *120*, 1021-1032.

Duarte, A., Hirashima, M., Benedito, R., Trindade, A., Diniz, P., Bekman, E., Costa, L., Henrique, D., and Rossant, J. (2004). Dosage-sensitive requirement for mouse Dll4 in artery development. Genes & development *18*, 2474-2478.

Ema, M., Takahashi, S., and Rossant, J. (2006). Deletion of the selection cassette, but not cis-acting elements, in targeted Flk1-lacZ allele reveals Flk1 expression in multipotent mesodermal progenitors. Blood *107*, 111-117.

Fish, J.E., Wythe, J.D., Xiao, T., Bruneau, B.G., Stainier, D.Y., Srivastava, D., and Woo, S. (2011). A Slit/miR-218/Robo regulatory loop is required during heart tube formation in zebrafish. Development *138*, 1409-1419.

Han, H., Tanigaki, K., Yamamoto, N., Kuroda, K., Yoshimoto, M., Nakahata, T., Ikuta, K., and Honjo, T. (2002). Inducible gene knockout of transcription factor recombination signal binding protein-J reveals its essential role in T versus B lineage decision. International immunology *14*, 637-645.

Jho, E.H., Zhang, T., Domon, C., Joo, C.K., Freund, J.N., and Costantini, F. (2002). Wnt/beta-catenin/Tcf signaling induces the transcription of Axin2, a negative regulator of the signaling pathway. Molecular and cellular biology *22*, 1172-1183.

Kothary, R., Clapoff, S., Darling, S., Perry, M.D., Moran, L.A., and Rossant, J. (1989). Inducible expression of an hsp68-lacZ hybrid gene in transgenic mice. Development *105*, 707-714.

Kuwajima, T., Sitko, A.A., Bhansali, P., Jurgens, C., Guido, W., and Mason, C. (2013). ClearT: a detergent- and solvent-free clearing method for neuronal and non-neuronal tissue. Development *140*, 1364-1368.

Liang, Y., Chang, J., Lynch, S.J., Lukac, D.M., and Ganem, D. (2002). The lytic switch protein of KSHV activates gene expression via functional interaction with RBP-Jkappa (CSL), the target of the Notch signaling pathway. Genes & development *16*, 1977-1989.

Liu, F., and Patient, R. (2008). Genome-wide analysis of the zebrafish ETS family identifies three genes required for hemangioblast differentiation or angiogenesis. Circ Res *103*, 1147-1154.

Lustig, B., Jerchow, B., Sachs, M., Weiler, S., Pietsch, T., Karsten, U., van de Wetering, M., Clevers, H., Schlag, P.M., Birchmeier, W.*, et al.* (2002). Negative feedback loop of Wnt signaling through upregulation of conductin/axin2 in colorectal and liver tumors. Mol Cell Biol *22*, 1184-1193.

Maretto, S., Cordenonsi, M., Dupont, S., Braghetta, P., Broccoli, V., Hassan, A.B., Volpin, D., Bressan, G.M., and Piccolo, S. (2003). Mapping Wnt/beta-catenin signaling during mouse development and in colorectal tumors. Proceedings of the National Academy of Sciences of the United States of America *100*, 3299-3304.

Mayor, C., Brudno, M., Schwartz, J.R., Poliakov, A., Rubin, E.M., Frazer, K.A., Pachter, L.S., and Dubchak, I. (2000). VISTA : visualizing global DNA sequence alignments of arbitrary length. Bioinformatics *16*, 1046-1047.

Murtaugh, L.C., Stanger, B.Z., Kwan, K.M., and Melton, D.A. (2003). Notch signaling controls multiple steps of pancreatic differentiation. Proc Natl Acad Sci U S A *100*, 14920-14925.

Muzumdar, M.D., Tasic, B., Miyamichi, K., Li, L., and Luo, L. (2007). A global double-fluorescent Cre reporter mouse. Genesis *45*, 593-605.

Nye, J.A., Petersen, J.M., Gunther, C.V., Jonsen, M.D., and Graves, B.J. (1992). Interaction of murine ets-1 with GGA-binding sites establishes the ETS domain as a new DNA-binding motif. Genes & development *6*, 975-990.

Ober, E.A., Olofsson, B., Makinen, T., Jin, S.W., Shoji, W., Koh, G.Y., Alitalo, K., and Stainier, D.Y. (2004). Vegfc is required for vascular development and endoderm morphogenesis in zebrafish. EMBO Rep *5*, 78-84.

Siekmann, A.F., and Lawson, N.D. (2007). Notch signalling limits angiogenic cell behaviour in developing zebrafish arteries. Nature *445*, 781-784.

Vijayaraj, P., Le Bras, A., Mitchell, N., Kondo, M., Juliao, S., Wasserman, M., Beeler, D., Spokes, K., Aird, W.C., Baldwin, H.S*., et al.* (2012). Erg is a crucial regulator of endocardial-mesenchymal transformation during cardiac valve morphogenesis. Development (Cambridge, England) *139*, 3973-3985.

Vong, L.H., Ragusa, M.J., and Schwarz, J.J. (2005). Generation of conditional Mef2cloxP/loxP mice for temporal- and tissue-specific analyses. Genesis *43*, 43-48.

Wythe, J.D., Jurynec, M.J., Urness, L.D., Jones, C.A., Sabeh, M.K., Werdich, A.A., Sato, M., Yost, H.J., Grunwald, D.J., Macrae, C.A*., et al.* (2011). Hadp1, a newly identified pleckstrin homology domain protein, is required for cardiac contractility in zebrafish. Disease models & mechanisms *4*, 607-621.